

UNIVERSITY OF CALIFORNIA

Los Angeles

High Voltage Time-dependent Dielectric Breakdown Study of Polyvinylidene Fluoride

Dielectric Films for a Flexible Electrostatic Energy Storage System

A thesis submitted in partial satisfaction of the requirements

for the degree Master of Science

in Materials Science and Engineering

by

Niharika Tripathi

2023

© Copyright by

Niharika Tripathi

2023

ABSTRACT OF THIS THESIS

High Voltage Time-dependent Dielectric Breakdown Study of Polyvinylidene Fluoride Dielectric Films for a Flexible Electrostatic Energy Storage System

by

Niharika Tripathi

Master of Science in Materials Science and Engineering

University of California, Los Angeles, 2023

Professor Subramanian Srikantes Iyer, Chair

In recent years, climate change has been an alarming issue and there is a pressing need for a greener, cost-effective, durable high-density energy storage system. This thesis investigates an electrostatic energy storage method using flexible roll-to-roll capacitors at very high voltages (5 kV – 10 kV) and investigates PVDF as a potential dielectric material for the capacitors. PVDF is chosen as a material due to its high dielectric constant, high dielectric breakdown strength, and low flexural modulus (high flexibility). Short-time stepped voltage ramp dielectric breakdown and the time-dependent dielectric breakdown for 75 μm PVDF films have been studied to understand the DC dielectric breakdown strength for the application of PVDF dielectrics under high voltage

stress for long periods of time. It has been shown that PVDF can withstand up to 10 kV and does not break down instantaneously. The failure rate dependence on electric field and temperature has been shown along with the prediction of the lifetime of PVDF dielectrics for a period of 10 years (100000 hours). It was found that a capacitor voltage range of 4000 V - 9200 V for a 100 μm PVDF dielectric film would lead to a time to failure of 10 years. The acceleration parameters and activation energy of PVDF films have also been shown to demonstrate the temperature dependence on TDDB of PVDF films. This thesis attempts an in-depth understanding of dielectric breakdown mechanisms, proposes, and investigates PVDF as a potential dielectric candidate, and analyzes the TDDB of polymer films using the thermochemical model (E model).

The thesis of Niharika Tripathi is approved.

Jaime Marian

Aaswath Pattabhi Raman

Subramanian Srikantes Iyer, Committee Chair

University of California, Los Angeles

2023

Dedicated to my parents.

TABLE OF CONTENTS

CHAPTER 1 INTRODUCTION.....	1
1.1 The demand for a new energy storage system.....	1
1.2 Dielectric breakdown mechanisms of polymers.....	3
1.3 The objective of this work.....	8
1.4 Organization of this thesis.....	9
CHAPTER 2 MATERIAL SELECTION AND SAMPLE PREPARATION.....	10
2.1 Materials selection for flexible capacitors.....	10
2.2 Overview and properties of PVDF.....	11
2.3 Sample preparation and electrode fabrication.....	13
CHAPTER 3 DIELECTRIC BREAKDOWN TESTING OF PVDF FILMS.....	15
3.1 Introduction to VRDB and TDDB testing.....	15
3.2 Experimental test setup.....	18
3.3 Experiment and results.....	20
3.3.1 VRDB testing of PVDF films.....	20
3.3.2 TDDB testing of PVDF films.....	22
3.3.2.1 Acceleration parameter as a function of temperature.....	23
3.3.2.2 Calculation of activation energy of the PVDF films.....	24
3.3.2.3 Lifetime prediction of capacitors using PVDF as a dielectric.....	25
CHAPTER 4 CONCLUSION AND FUTURE WORK.....	26
REFERENCES.....	28

LIST OF FIGURES

Figure 1-1 Schematic of an electrostatic energy storage system with rollable high-voltage large-volume capacitors stored locally in a distributed manner.....	3
Figure 1-2 Energy band diagram showing the defect generation process in Llyod model.....	5
Figure 1-3 Si-Si bond breaking under voltage stress in the E model.....	5
Figure 1-4 Anode Hole Injection mechanism in 1/E model.....	6
Figure 1-5 Electrical treeing in a polymer dielectric film.....	8
Figure 2-1 PVDF polymer chain structure.....	12
Figure 2-2 α , β , and γ morphologies of PVDF.....	13
Figure 2-3 Screen-printed silver epoxy electrodes on (a) 125 μm and (b) 75 μm PVDF films.....	14
Figure 2-4 NeoDen screen printer used for screen printing electrodes.....	14
Figure 3-1 Comparison of time-to-failure extrapolation of E vs. 1/E model.....	18
Figure 3-2 Schematic of the test set-up used for breakdown testing of PVDF samples.....	19
Figure 3-3 (a) Front view of the experimental test set-up. Left to right: Test fixture with a PVDF sample in a petri dish and the high voltage DC power supply (b) PVDF sample dielectric breakdown tested in an insulating oil medium.....	20
Figure 3-4 Voltage Ramp Dielectric Breakdown test profile.....	21
Figure 3-5 Time-to-failure vs. Electric field at $T = 298 \text{ K}$ and 318 K	23

Figure 3-6 Time-to-failure vs. $1/T$ at $T = 318\text{ K}$, 328 K and 338 K24

Figure 3-7 Plot of $\log(\text{time to failure})$ vs. electric field and extrapolation of lifetime assuming the 'E model'25

LIST OF TABLES

Table 1-1 Dimensions of the rolled-up capacitor.....	2
Table 1-2 Types of breakdown for polymer dielectrics with time and effect.....	7
Table 2-1 Breakdown strengths, dielectric constants, and flexural modulus of various polymers..	11
Table 3-1 Design of Experiment for TDDB testing of PVDF films.....	22

ACKNOWLEDGEMENTS

Firstly, I would like to thank my advisor Prof. Subramanian S. Iyer for being my mentor and guiding me throughout this project. Professor Iyer's knowledge and support have been immensely helpful in my graduate journey.

I would also like to thank Professor Jaime Marian and Professor Aaswath Raman for being my thesis committee members and giving their valuable time.

I would like to thank my mentors, Randall Irwin, Goutham Ezhilarasu, Tak Fukushima and colleagues at CHIPS lab, Tianyu Xiang, Harshit Ranjan, and for assisting me and helping me throughout my research project. I sincerely thank all my lab members for being so encouraging and providing a constructive environment.

I would also like to take this opportunity to thank my departmental graduate advisor, Kyle, for helping me out selflessly and providing me with valuable advice during my difficult times.

I would finally like to thank my family and friends for their unconditional love and support. I could not have done this without them.

CHAPTER 1: INTRODUCTION

1.1 The demand for a new energy storage system

Currently, the most common energy storage systems are mechanical (flywheels, storage tanks) and electrochemical (batteries). The intermittent nature of renewable energy sources (solar and wind) requires long-term energy storage for which current energy storage systems such as Li-ion batteries are unsuitable due to their high costs (\$151/kWh) per kWh of energy stored [1]. In addition, the previously stated approaches to storing energy either lack a method for electricity storage with zero waste or require a centralized electrical grid. With the climate changing due to greenhouse gas emissions, there is an urgent need for a greener, more cost-effective long-duration energy storage system [2].

Figure 1-1 shows a proposed method of an electrostatic energy storage system which is an environmentally friendly high-density energy storage system made up of flexible rolled-up capacitors which store energy at very high voltages (5 kV - 10 kV). It can be distributed underground to supply electrical energy locally (households), which is also cost-effective.

This method utilizes an intermittent power input at a low voltage which is converted to a higher voltage using a high-efficiency power converter. This high voltage is then used to store charge on flexible, tightly wound capacitor cells with the dimensions mentioned in Table 1-1 below. This high voltage on the capacitor can then be converted to a lower voltage as per the application.

Dimension of the cell	Units (mm)
Height	1000
Outer Diameter	1000
Inner Diameter	200
Number of turns	1000
Turn spacing	0.2

Table 1-1 Dimensions of the rolled-up capacitor.

The energy stored in a capacitor is given by the following equation: $E = \frac{1}{2} CV^2$, where E is the energy stored, C is the capacitance and V is the voltage.

The capacitance is given by the equation: $C = \frac{k\epsilon_0 A}{d}$, where k is the dielectric constant of the dielectric, ϵ_0 is the permittivity of the vacuum, A is the area of the capacitor, and d is the distance between the electrodes (thickness of the dielectric film). Therefore, we can directly increase the electrostatic energy stored by either choosing a material with a high dielectric constant, increasing the voltage applied, increasing the area of the electrode, decreasing the film thickness, or some combination of these. From the formulae mentioned above, we can derive that the electrostatic energy stored linearly depends on the dielectric constant of the dielectric, area of the electrodes, and the voltage across the electrodes, under a constant field. The equation that shows this relationship is: $E = \frac{1}{2} k\epsilon_0 A \left(\frac{V}{d}\right) V$. The field depends on both the voltage applied as well as the thickness of the dielectric layer.

The flexible, rolled capacitors required for this electrostatic energy storage system need to have dielectrics that can withstand these high voltages over longer periods of time. The next section

provides a brief overview of the mechanisms by which dielectrics break down, mainly considering polymers as the materials of choice.

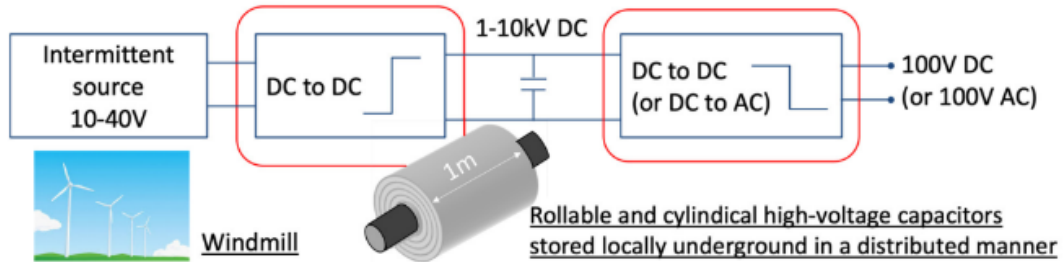


Figure 1-1 Schematic of an electrostatic energy storage system with rollable high-voltage large-volume capacitors stored locally in a distributed manner.

1.2 Dielectric breakdown mechanisms of Polymers

Maximizing capacitor energy density involves applying very high voltages across the capacitor. Thus, understanding the dielectric strength and breakdown mechanisms of the material is crucial prior to selection. Dielectric breakdown mechanisms also help in understanding the reliability and lifetime of devices.

The breakdown of a dielectric material occurs when the material loses its insulating properties and starts conducting when placed under high electric fields or voltage stresses. The underlying breakdown mechanisms of various dielectrics have been studied extensively for decades. Broadly, the breakdown can be classified into two types: intrinsic and extrinsic. The intrinsic breakdown can further be categorized as thermal, avalanche, or electro-mechanical breakdown [3]–[6]. Extrinsic breakdown occurs due to macroscopic defects or defects induced due to external factors such as stacking faults, whereas intrinsic breakdown is due to the intrinsic defects present in the material such as point defects, vacancies, etc. assuming there are no external defects or impurities [7].

The extrinsic breakdown can be minimized by using clean processes and processing environments. The intrinsic breakdown, however, is a property of the material itself and depends on factors such as voltage stress, the thickness of the material, temperature, time, etc. This section delves deep into the dielectric breakdown mechanisms of solid insulators and of polymers such as PVDF.

For solid dielectrics, three major models have been proposed: The Llyod model (also known as the \sqrt{E} model), the E model (Thermomechanical model), and the $1/E$ model, also known as the Anode Hole Injection Model (AHI model) as shown by Lombardo S. et. al. [7] [8] The Llyod model is a theoretical model which interprets inelastic collision of energetic electrons as the cause for breakdown. This model assumes that electrons are injected via the Poole-Frenkel emission and [9] after injection, the electrons are accelerated and acquire energy due to the electric field. If the energy acquired is greater than the threshold energy, it can generate a new defect, and the accumulation of these defects can lead to a breakdown. Figure 1-2 shows the energy band diagram of a low-k dielectric material, explaining how energetic electrons can lead to new defects or trap generation [10].

The E model, also known as the Thermomechanical model, is a molecular model that attributes the cause of dielectric breakdown to be the breakage of weak bonds due to the applied electric field, which further leads to defects such as trap generation [11]. Figure 1-3 shows a schematic of the E' centers in SiO_2 gate oxides which is an oxygen vacancy defect, where two Si atoms form a bond with each other and are also attached to three other oxygen atoms. The E model suggests that under high electric field stress, Si-Si bonds will break as they have a lower bond energy (1.8 eV) when compared to Si-O bonds (5.4 eV), and when enough defects are generated, breakdown will occur [12].

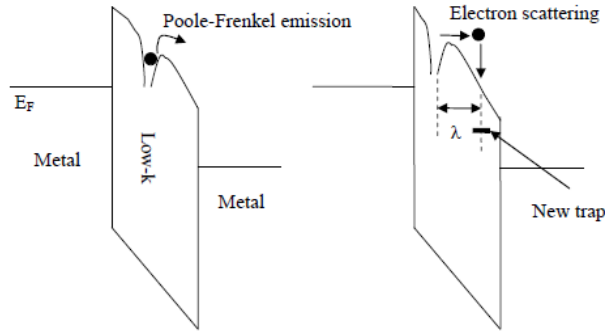


Figure 1-2 Energy band diagram showing the defect generation process in Lloyd model. [8]

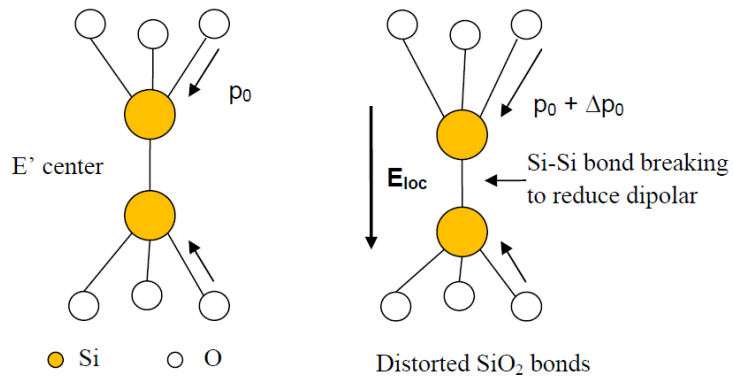


Figure 1-3 Si-Si bond breaking under voltage stress in the E model [8]

The third model, which is the $1/E$ model or AHI model, or Substrate Hole Injection model is illustrated in Figure 1-4. This mechanism considers the high electric field across the oxide to produce energetic electrons that tunnel across via Fowler-Nordheim tunneling. These high-energy electrons thermalize when they reach the anode and generate holes. Due to the direction of the applied electric field, the holes travel back across the dielectric but get trapped as they are heavier [13] These defects will build up and keep increasing the electric field near the cathode, which will lead more electrons to traverse across the oxide and this will follow a feedback loop.

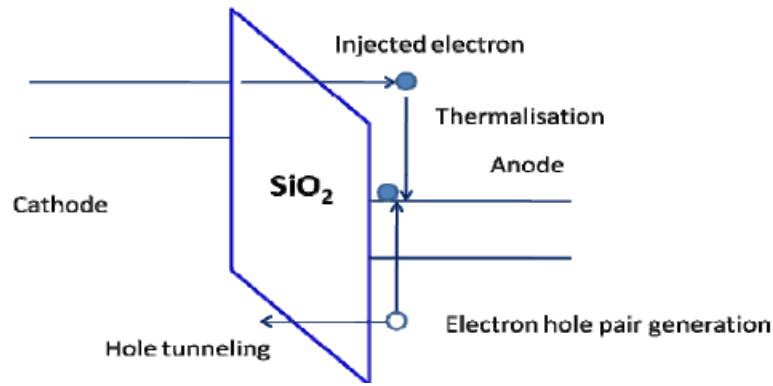


Figure 1-4 Anode Hole Injection Mechanism in I/E model [8]

In all the above-mentioned mechanisms, defect generation can lead to a soft or hard breakdown. Soft breakdown is caused when a weak spot starts leaking current but not to a limit when breakdown occurs, and the material loses all its insulating properties. However, a hard breakdown occurs when enough defects are generated, and these accumulate to form a bridge between the two electrodes and form a percolation path that ultimately leads to the breakdown of the material, and the dielectric starts conducting [14].

Polymers share some similarities in the way they break down with ceramics but are also different in terms of their structure and dielectric properties. The breakdown mechanisms in polymers, depending on whether they are instantaneous or time-dependent, can be of two types: short-term breakdown, which occurs at higher voltages instantaneously in the range of nanoseconds to milliseconds, and long-term breakdown, which occurs over long periods of time at low voltages. Table 1-2 shows an overview of the types of breakdown that occur in polymers along with the general time to breakdown and effects they can have on the dielectric [15][16][17].

Fast or short-term avalanche breakdown can occur at a lower temperature, whereas electromechanical breakdown can occur at higher temperatures. Short-term avalanche breakdown

occurs when electrons gain energy due to electric fields and this energy is greater than the energy lost when they interact with phonons. These energetic electrons gain kinetic energy and, due to impact ionization, generate more electrons which are also accelerated under the electric field and the process repeats. Electromechanical breakdown occurs when the mechanical properties of the polymer change. In this type of breakdown, electrostatic attraction of the electrodes takes place, and depending on Young's modulus of the polymer, the width of the insulation decreases. For the same applied voltage, the field thus increases with a decrease in thickness. The effect worsens with local heating and increases softening in the region of thickness reduction. The thermal breakdown usually is a combination of both and occurs at an intermediate temperature range. These short-term breakdown mechanisms usually occur under higher voltage stresses and within a short span of time [18].

	Mechanism	Time to breakdown	Effect
Short-term	Avalanche	$10^{-9} - 10^{-6}$ s	Catastrophic: dielectric loses all insulating properties
	Thermal	$10^{-7} - 10^{-3}$ s	
	Electromechanical	$10^{-6} - 10^{-3}$ s	
Long-term	Electrical trees	$10^2 - 10^7$ s	Reduces breakdown voltage: may lead to a breakdown
	Water trees	hours - years	
	Partial discharge	hours - years	

Table 1-2 Types of breakdown for polymer dielectrics with time and effect.

Long-term breakdown or degradation in polymers occurs when much lower voltages are applied to the dielectric but for a long period of time. Electrical or water trees are similar to fast avalanches, as they also occur due to energetic electrons, but the conduction path is formed slowly. Partial discharges occur due to voids or defects in the material when there are electrical discharges, and these can further cause local heating which could lead to thermal breakdown over time [18].

Figure 1-5 shows a diagram of how electrical trees form in the dielectric film under high voltage stress due to defect formation.

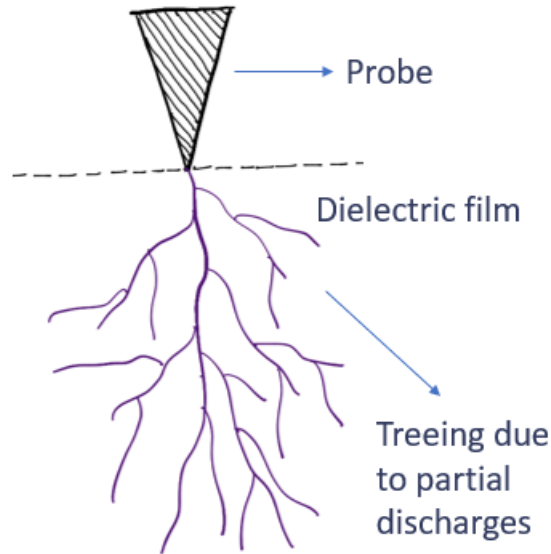


Figure 1-5 Electrical treeing in a polymer dielectric film.

Breakdown mechanisms can dominate under different conditions: voltage stress, time, temperature, type of defect, or polymer structure. To fully understand the conditions at which a material breaks down and the cause of the breakdown, voltage-ramp dielectric breakdown (VRDB) and Time-dependent dielectric breakdown (TDDB) tests can be performed at accelerated conditions, and the samples can then be inspected and analyzed to predict the lifetime under real conditions. These tests will be elaborated on in Chapter 3.

1.3 Objective of this thesis

Although dielectric breakdown studies have been performed on various dielectrics [8], [19]–[21], the dielectric behavior for flexible polymer dielectrics at very high voltages has not been

studied in detail. The objective of this thesis is to focus on the breakdown mechanisms and behavior of PVDF under high DC voltage stresses over long periods of time.

The main deliverables of this thesis are:

- 1) Material selection for a flexible high-density electrostatic energy storage system.
- 2) Performing VRDB and TDDB tests on PVDF samples to understand the influence of voltage stress and temperature on time-to-failure.
- 3) Predict the lifetime of roll-to-roll capacitors with PVDF as the dielectric and the corresponding operating voltage.

1.4 Organization of this thesis

The first chapter of this thesis is an introduction to the need for a new energy storage system and an understanding of the dielectric breakdown mechanisms of polymers. The second chapter delves deep into the process of material selection of PVDF as a potential dielectric candidate and the sample preparation. In Chapter 3, the experimental setup and results of the VRDB and TDDB tests are given. Chapter 4 concludes this thesis along with some future work that can be carried out.

CHAPTER 2: MATERIAL SELECTION AND SAMPLE PREPARATION

2.1. Materials selection for high energy-density flexible capacitors

As in the proposed electrostatic energy storage system, the capacitors will be rolled into compact cells, therefore the dielectric material chosen should be thin and flexible. In addition, it must have a high dielectric constant to maximize energy density and breakdown strength to maximize tolerable voltage.

Compared to ceramic dielectrics, polymer films have a major advantage in handling, ease of processing, and higher breakdown strength [22]. Table 2-1 shows the dielectric constant and breakdown strength of various polymer dielectric candidates. PVDF is a polymer with both a high dielectric constant k (6-10) and high breakdown strength (>700 V/ μm) [23]–[28]. Additionally, PVDF also possesses a lower flexural modulus (1.5-2 GPa) compared to other polymers giving it higher flexibility. Table 2-1 also shows the values of the flexural modulus of some polymers. Although PTFE and PP have a lower flexural modulus, they lack a high dielectric constant, when compared to PVDF which would overall lead to a reduced energy stored.

For the electrostatic energy storage application, a dielectric material is required that has an optimal balance of high dielectric breakdown strength, high dielectric constant, and high flexibility (low flexural modulus). PVDF is chosen as a potential candidate and further investigations have been done on prototypes that will be discussed in Chapter 3. The next section gives an overview of the structure and morphologies of PVDF along with its properties.

Properties	DC breakdown strength (V/ μm)	Dielectric constant	Flexural modulus (GPa)
PVDF (polyvinylidene fluoride)	590 ^[26] , 720-770 ^[24]	10.2 (10 Hz) ^[24] 8.4 (60Hz) ^[29] 7.7 (1kHz) ^[29] 6.4 (1MHz) ^[29]	1.5-2 ^[30]
HDPE (high-density polyethylene)	600 ^[31]	2.30-2.35 (1MHz) ^[32]	0.75-1.5 ^[30]
LDPE (low-density polyethylene)	650 ^[27]	2.25-2.35 (1MHz) ^[32]	0.15-2.2 ^[33]
PC (polycarbonate)	528 ^[27] , 720 ^[26]	2.8 (1MHz) ^[34]	2.2-2.5 ^[30]
PET (polyethylene terephthalate)	420-460 ^[35] (660-750) ^[35]	3.25 (1kHz) ^[34] 3 (1 MHz) ^[34] 2.8 (1 GHz) ^[34]	2.8-3 ^[30]
PI (polyimide)	470 ^[26] , 600-650 ^[25]	3.6 (100 Hz) ^[26] 3.4 (1kHz) ^[23] 3.3 (1MHz) ^[23] 3.2 (1GHz) ^[23]	1.38-40 ^[36]
PP (polypropylene)	640 ^[28] , 500-800 ^[25]	2.2-2.6 (1MHz) ^[34]	1.2-1.6 ^[30]
PS (polystyrene)	600 ^[27] , 450 ^[26]	2.4-2.7 (1MHz) ^[34]	2.5-3.5 ^[30]
PTFE (polytetrafluoroethylene)	400-800 ^[25]	2.1 (1kHz & 1MHz) ^[32]	0.4-0.8 ^[30]

Table 2-1 Breakdown strengths, dielectric constants, and flexural modulus of various polymers.

2.2. Overview and properties of PVDF

Polyvinylidene fluoride (PVDF) is an organic fluoropolymer that exhibits excellent mechanical and thermal properties along with a high dielectric constant and dielectric breakdown strength [37]. It is made up of the repeating units of the monomer $-(\text{CH}_2\text{-CF}_2)_n-$ and the molecular structure of PVDF can be seen in Figure 2-1 [38].

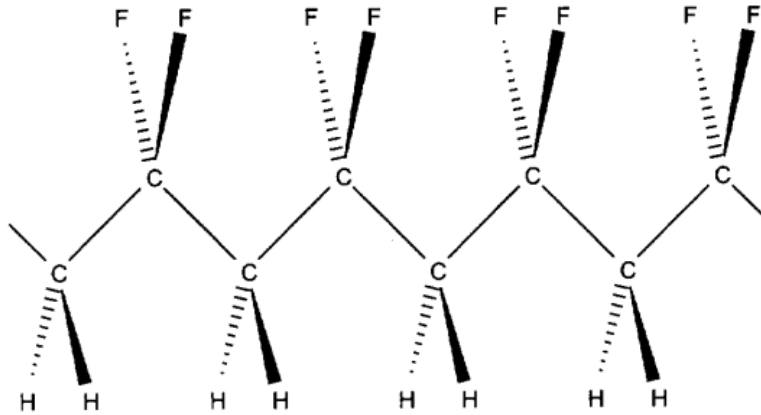


Figure 2-1 PVDF polymer chain structure [38]

The PVDF molecular structure can be of three types depending on polarity: α -PVDF which is non-polar, β -PVDF which is polar, and γ -PVDF which is moderately polar. FTIR studies have been performed over time to differentiate these phases [39]. The β -phase of PVDF typically shows a higher breakdown strength than the α -phase, due to its conformation which leads to spontaneous polarization upon the application of an electric field [40]. Figure 2-2 shows the α , β , and γ morphologies of PVDF. Generally, the PVDF films commercially obtained are in the α -phase and when strained or stretched, mechanically, electrically, or thermally, they transform to the β -phase which is electroactive and polar [41].

As can be seen from Figure 2-2, the β -phase has a zig-zag structure that follows a TTTT conformation (trans), and the dipole moments of these β chains have a parallel dipole orientation as the dipole moments point in the same direction. The β -phase of PVDF is not very stable as there is an overlap between the fluorine atoms due to the reduced space available around them. The γ -phase, however, takes form when the stress conditions are moderate (mechanical, thermal, or electrical) [40].

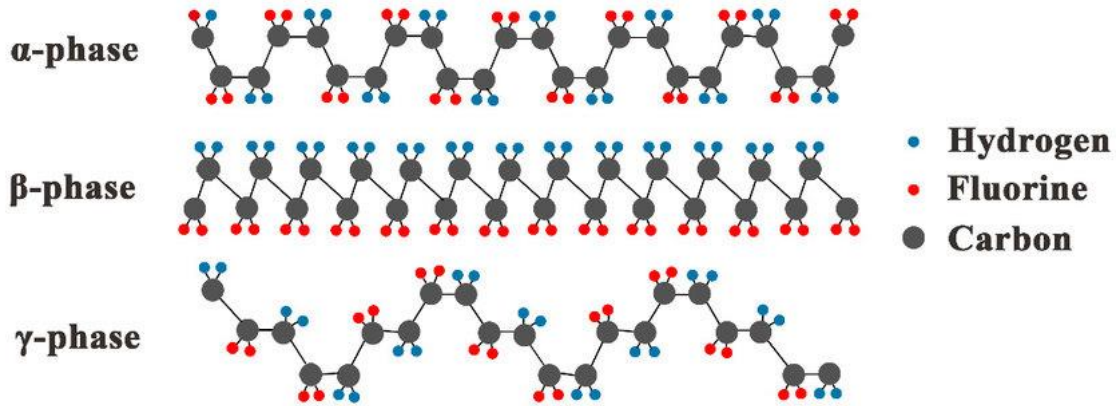


Figure 2-2 α , β , and γ morphologies of PVDF [42].

As in this study, PVDF films are being employed which need to be used at high voltage conditions, there can be transformations within these three morphologies depending on the voltage stress limits and the thermal stresses produced due to the same. The sample preparation and electrode fabrication on PVDF films has been discussed in the next section.

2.3. Sample preparation and electrode fabrication

PVDF (Kynar[®]) films of two thicknesses (75 μm and 125 μm) were obtained from CS Hyde [43]. Figure 2-3 shows the top electrodes of different sizes that were fabricated over both films using screen printing. Figure 2-4 shows the NeoDen screen printer that was used for this purpose. The back sides of both films were coated completely which acts as the bottom electrode. Four different electrode areas were screen-printed using a silver epoxy paste: 1mm x 1mm, 2mm x 2mm, 5mm x 5mm, and 10mm x 10mm. The electrodes with an area of 5 mm x 5 mm were then broken apart and used as test samples.

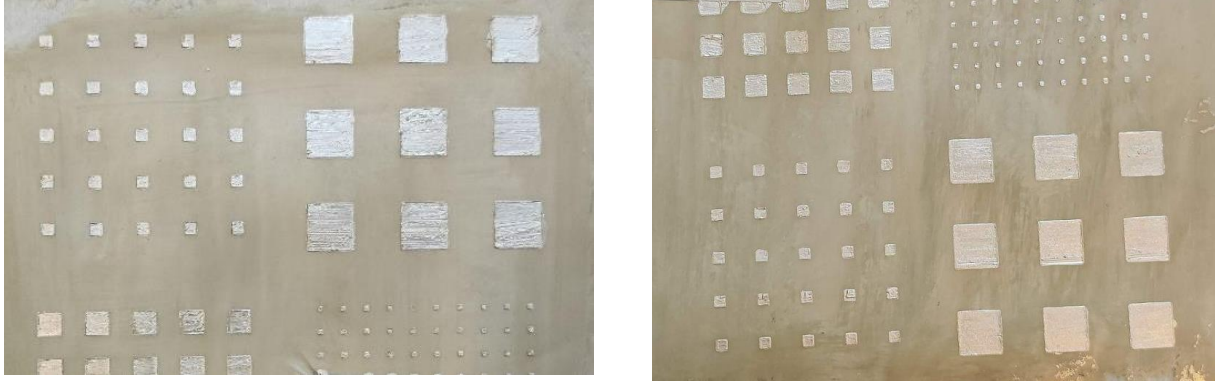


Figure 2-3 Screen-printed silver epoxy electrodes on (a) 125 μm and (b) 75 μm PVDF films.

It has previously been shown that a smaller electrode size has higher breakdown strength due to reduced extrinsic impurities. However, these studies have been conducted for AC voltage testing [44], [45]. It is also believed that a thicker film has a higher breakdown strength, but this cannot be generalized as it majorly depends on the dielectric material and the mechanism of breakdown [3], [7].

The next chapter introduces Voltage Ramp Dielectric Breakdown testing and Time-Dependent Dielectric Breakdown testing, discusses the experiments that were performed on the PVDF samples, and provides an analysis of the results that were obtained from the experiments.



Figure 2-4 NeoDen screen printer used for screen printing electrodes.

CHAPTER 3: DIELECTRIC BREAKDOWN TESTING OF PVDF FILMS

3.1. Introduction to Voltage Ramp Dielectric Breakdown (VRDB) testing and Time-dependent dielectric breakdown testing (TDDB)

A capacitor when placed under voltage stress exceeding a critical value will break down – this can be instantaneous or over time. To test the immediate breakdown of capacitors (dielectrics), a testing method known as Voltage Ramp Dielectric Breakdown (VRDB) can be used. In this method, the voltage applied to the dielectric test sample is ramped either linearly or as a stepped function. The breakdown voltage (V_{bd}) is measured as soon as there is an abrupt increase in leakage currents. For a stepped voltage ramp test, the output voltage V_{step} applied is stepped at regular intervals where each step is held for a holding time t_{step} [46]. According to the JEDEC standard JEP159A, the dielectric voltage to breakdown (V_{bd}) and the dielectric breakdown current (I_{bd}) should be recorded and analyzed. The criterion for dielectric breakdown is fulfilled when there is an abrupt increase in dielectric current.

Post VRDB test, a Weibull or normal distribution can be used to fit the results and derive the scale parameter of the V_{bd} Weibull distribution (V_{bd63}) and the shape factor of the distribution (β of V_{bd}). The scale parameter of a Weibull distribution (t_{bd63}) and the shape factor (β of t_{bd}) can be analyzed from the distribution plots for the lifetime prediction of devices that will be used for real-time application. The probability distribution function (pdf) equation of a distribution can be used for understanding reliability. The pdf of a Weibull distribution is given by: $f(x) =$

$\frac{\beta}{\eta} \left(\frac{x-\gamma}{\eta}\right)^{\beta-1} e^{-\left(\frac{x-\gamma}{\eta}\right)^\beta}$, where β is the shape parameter, γ is the location parameter and η is the scale parameter. The pdf of a normal distribution is given by: $f(x) = \frac{1}{\sigma\sqrt{2\pi}} e^{-\frac{1}{2}\left(\frac{x-\mu}{\sigma}\right)^2}$, where σ is the

standard deviation and μ is the mean. Visual inspection and failure analysis are also recommended on test samples after the breakdown has occurred. Microscopy can help with the visualization of breakdown spots throughout the sample.

Time-dependent dielectric breakdown is a reliability testing method to evaluate the lifetime of devices. In this method of testing, a constant stress voltage (V_{stress}) or field, which is less than the breakdown strength of the dielectric is supplied to the device under test (DUT) and the time to breakdown (t_{bd}) is measured along with the dielectric breakdown current (I_{bd}) [47]. A breakdown occurs when there is an abrupt increase in leakage currents and the dielectric becomes conductive.

The most common TDDB models are based on degradation induced by field, current, or a combination of the two. The three models, which are E, 1/E, and \sqrt{E} model show different correlations between time to failure (TTF) and the applied field.

According to the E model, the correlation between the time to failure and the electric field can be given by the following equation: [47]

$$TTF = A. \exp \left[\frac{\Delta H_0}{K_B T} - \gamma E \right]$$

where A is a constant, ΔH_0 is the activation energy (sometimes referred to as activation enthalpy), K_B is the Boltzmann constant, T is the temperature, γ is the acceleration parameter and E is the applied field through the dielectric. Taking the natural log of both sides for the above equation, we get: $\ln(TTF) = \ln A + \frac{\Delta H_0}{K_B T} - \gamma E$. The acceleration parameter γ at a constant temperature is then given by

$$\gamma = -\frac{\partial \ln(TTF)}{\partial E}$$

The activation energy can be given by:

$$\frac{\Delta H_0}{K_B} = \frac{\partial \ln(TTF)}{\partial \left(\frac{1}{T}\right)}$$

According to the \sqrt{E} model, the time to failure (TTF) can be expressed as

$$TTF = B \cdot \exp\left(\frac{\Delta H_0}{K_B T} - \gamma \sqrt{E}\right)$$

where B is a constant, γ is the acceleration factor and E is the field [48].

As per the 1/E model, the time to failure is inversely proportional to the field across the dielectric. As this is a current-based model, the time to failure shows a dependence exponentially on the reciprocal of the electric field, given by the equation below: [49]

$$TTF = \tau_0(T) \cdot \exp\left(\frac{G(T)}{E}\right)$$

where τ_0 is a temperature-dependent constant, G(T) is a factor associated with the electron and hole tunneling, and E is the electric field applied across the dielectric film.

Out of all the three models, the E model assumes breakdown due to bond ionization and provides the worst case for failure rate and time-to-failure. For this reason, we will assume the E model for predicting lifetime and time-to-failure (in hours) of the PVDF films tested. Figure 3-1 shows the comparison of time-to-failure trends of the E and 1/E models [47].

Trap/defect generation or bond breakage is considered to be responsible for time-dependent dielectric breakdown for solid dielectrics. The major mechanisms that lead to the

degradation of the dielectrics can be hydrogen-ion release; bond stretching and breaking due to applied field and local thermal stresses; and impact ionization due to leakage currents [50].

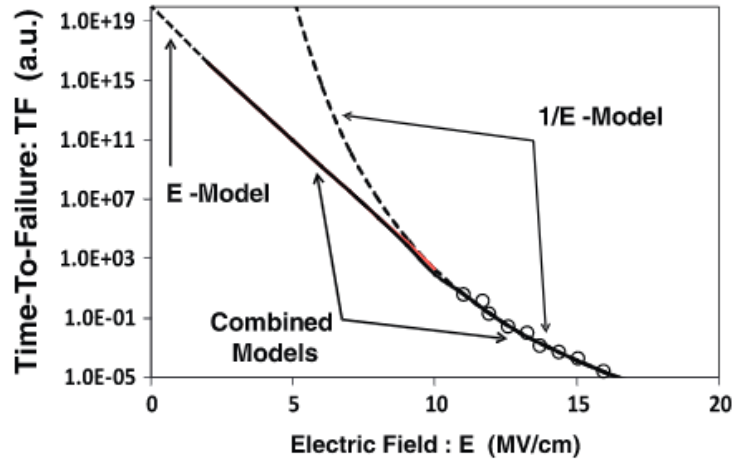


Figure 3-1 Comparison of time-to-failure extrapolation of E vs. 1/E model [47].

3.2. Experimental test set-up

Figure 3-2 shows the schematic of the test set-up used for both VRDB and TDDB tests of PVDF samples along with the wiring of the set up. The components of the test set-up are as follows:

1. Keithley 2290-10 High Voltage Power Supply
2. 10kV SHV male connection to 10kV banana 1.5-meter cable
3. Interlock cables
4. PVDF dielectric samples with printed Ag electrodes (Planar)
5. 10 kV high voltage test fixture box (PPD3 -10kV)
6. Insulating oil (mineral oil)
7. GPIB cable
8. Controller (laptop)

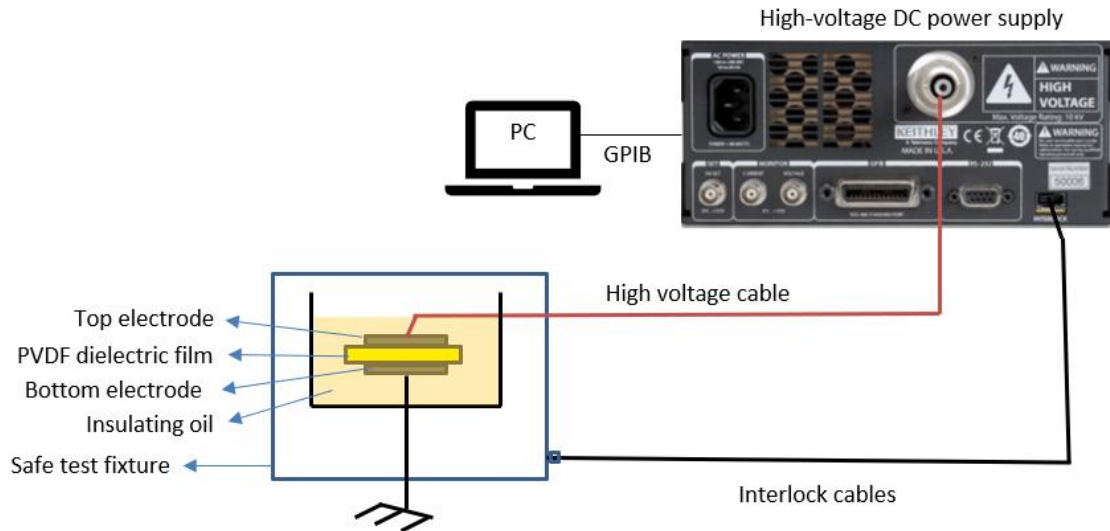


Figure 3-2 Schematic of the test set-up used for breakdown testing of PVDF samples.

The high-voltage power supply is connected to a safely grounded test fixture via a high-voltage cable. The PVDF samples are placed in a petri dish which is safely enclosed in the test fixture and kept in place using clamps provided in the test fixture. The PVDF samples are surrounded by oil to prevent arcing between the electrodes through the air around them. The power supply is controlled using a laptop which is connected via a National Instruments (NI) GPIB cable. NI Measurement and Automation Explorer (NI MAX) is used to establish basic communication with the power supply. The power supply sends signals using interlock cables, which seal the test fixture as soon as the output voltage supply is turned on. Figure 3-3(a) shows the actual set-up which was used for testing.

The high-voltage power supply can output DC voltage from 0-10000 V with ± 1 V and can measure output currents up to 1 mA with a $1 \mu\text{A}$ resolution. The output voltage is supplied through the high-voltage cable. The output voltage is supplied to the top electrode of the PVDF sample via a high-voltage test lead with an alligator clip. The sample is grounded using a wire with an alligator

clip connected to one of the pins of the test fixture (chassis ground). A close-up image of the PVDF sample under the test can be seen in Figure 3-3(b). The top and bottom electrodes of the film are connected to wires using silver epoxy paste.

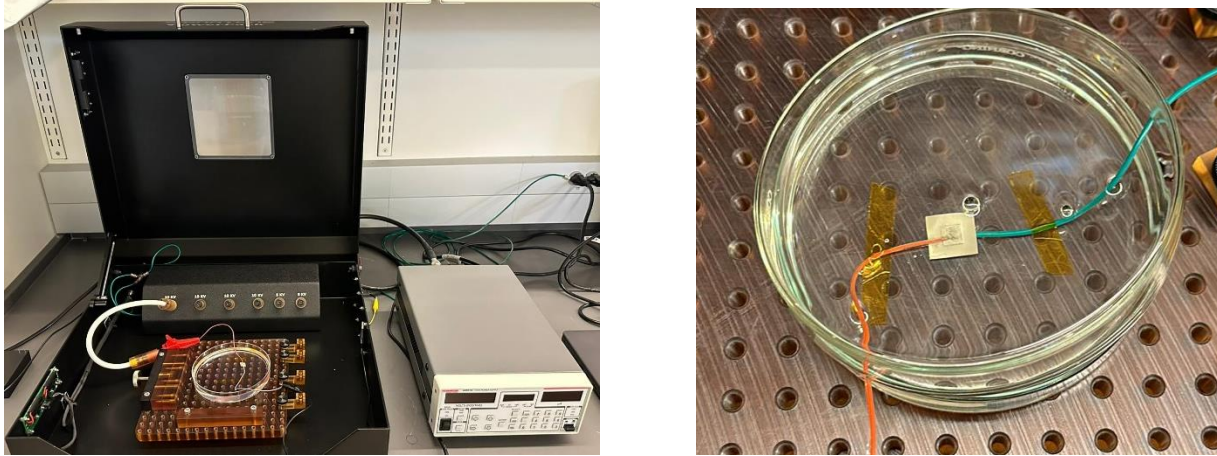


Figure 3-3 (a) Front view of the experimental test set-up. Left to right: Test fixture with a PVDF sample in a petri dish and the high voltage DC power supply (b) PVDF sample dielectric breakdown tested in an insulating oil medium.

3.3. Experiments and results

3.3.1. VRDB testing of the PVDF films

Stepped voltage ramp dielectric breakdown tests were performed on 10 different 75 μm -thick PVDF dielectric samples with an electrode area of 25 mm^2 . The step voltage ramp test profile is shown in Figure 3-4. The ramp rate used for this purpose was 1000 V/10s from 0-10000 V. All the samples were stable and PVDF did not break down up to 10 kV. The leakage currents observed were all under 1 μA , which is the minimum resolution of the power supply source. The step time of 10 seconds accounts for the holding time at a voltage plus the settling time for transient currents.

These short-time tests indicate that the dielectric's breakdown field is greater than 133.33 MV/m (or V/ μm). All the samples tested for VRDB were performed at room temperature and only voltage stress was ramped up for fixed time intervals. This shows that PVDF is stable under voltage stresses up to 10 kV keeping time and temperature constant.

Though the PVDF dielectric films didn't break down up to 10 kV in the short time tests, it is important to observe and record how these films behave under high voltage stress over long periods of time. The next section discusses the time-dependent dielectric breakdown tests performed on PVDF samples and the time to failure for the same.

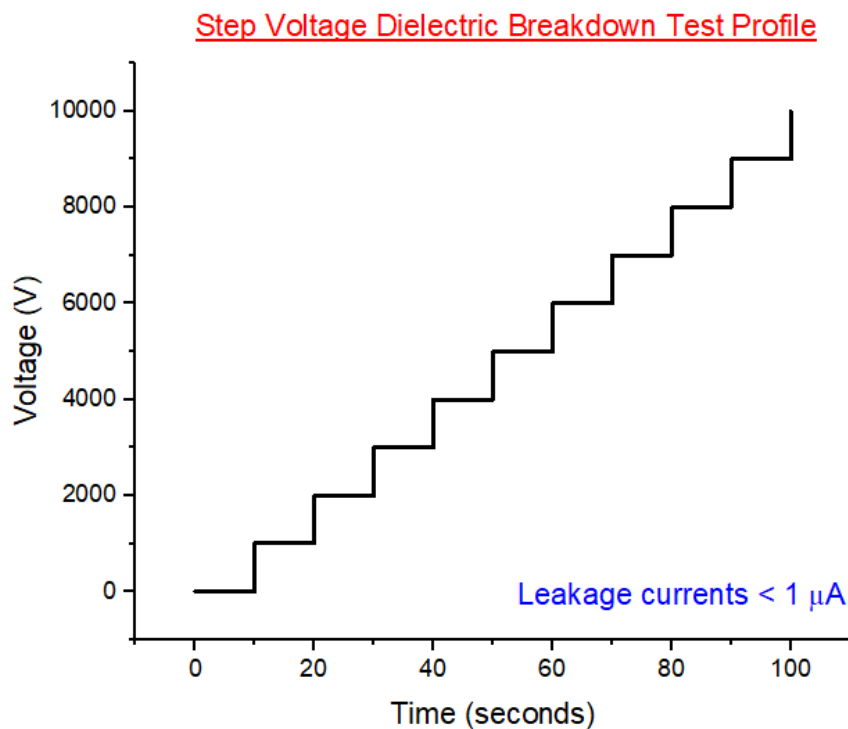


Figure 3-4 Voltage Ramp Dielectric Breakdown test profile.

3.3.2. TDDB testing of the PVDF films

For the time-dependent dielectric breakdown testing of PVDF films, the influence of voltage stress on time to failure was observed keeping the temperature constant as well as the influence of temperature keeping the voltage stress constant. Table 3-1 illustrates the design of experiments developed for studying the TDDB of different samples of 75 μm PVDF films with an electrode area of 25 mm^2 , by varying either the temperature or the voltage stress. The time to failure was observed and recorded for each of these trials, which is discussed in the latter sections. The criterion for the breakdown of the failed samples was leakage currents greater than 1 μA across the dielectric sample.

Trial #	Voltage (V)	Electric Field (MV/m)	Temperature (K)
1	10000	133.33	298
2	10000	133.33	298
3	9500	126.67	298
4	9000	120	298
5	8000	106.67	298
6	5000	66.67	318
7	6000	80	318
8	7000	93.33	318
9	7000	93.33	328
10	7000	93.33	338

Table 3-1 Design of Experiment for TDDB testing of PVDF films.

3.3.2.1. Acceleration parameter as a function of temperature

As seen in 3.3.1, the acceleration parameter is given by the relation: $\gamma = -\frac{\partial \ln(TTF)}{\partial E}$. The acceleration parameter helps us in understanding the influence of temperature on the failure rate of the dielectric material. The time-to-failure (in hours) for trials #1-8 were plotted against the electric field across the dielectric. Figure 3-5 shows the plot of log (time-to-failure) vs. the electric field applied across the dielectric layer. The acceleration parameters of both linear fits at temperatures of 298 K and 318 K are also shown on the graph, which is the negative value of the slopes. As can be seen from the graph, the acceleration parameter, γ_1 at $T = 298$ K comes out to be 0.08 (MV/m)^{-1} and γ_2 at $T = 318$ K comes out to be 0.04 (MV/m)^{-1} . As we can see, the failure rate increases with temperature as the time to failure reduces with temperature.

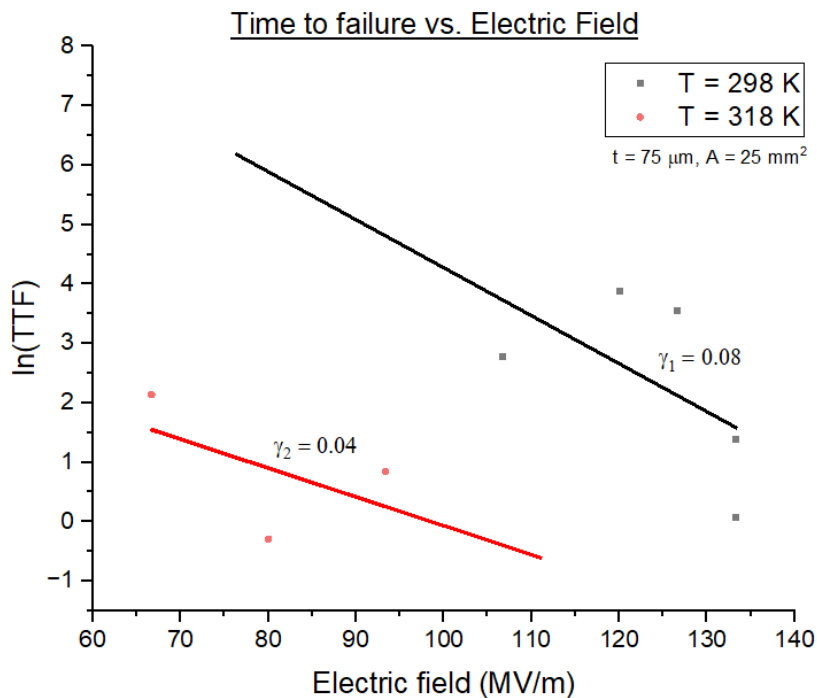


Figure 3-5 Time-to-failure vs. Electric field at $T = 298$ K and 318 K

3.3.2.2. Calculation of activation energy of the PVDF films

The activation energy is related to the temperature and time to failure by the equation:

$$\frac{\Delta H_0}{K_B} = \frac{\partial \ln(TTF)}{\partial \left(\frac{1}{T}\right)}$$

The activation energy, ΔH_0 gives an understanding of the nucleation of defects at a certain voltage stress. The time-to-failure (in hours) for trials #8-10 were plotted against the inverse of the temperature ($1/T$). Figure 3-6 shows the plot of $\ln(\text{time-to-failure})$ vs. inverse of temperature applied across the dielectric layer at a constant electric field of 93 MV/m.

The slope of the graph gives the value of $\Delta H_0/K_B$, for an applied field of 93 MV/m and it comes out to be 10088 which is $\sim 10^4$ K. The activation energy then can be calculated as $10^4 \times K_B = 1.38 \times 10^{-19}$ J, which is 0.8625 eV.

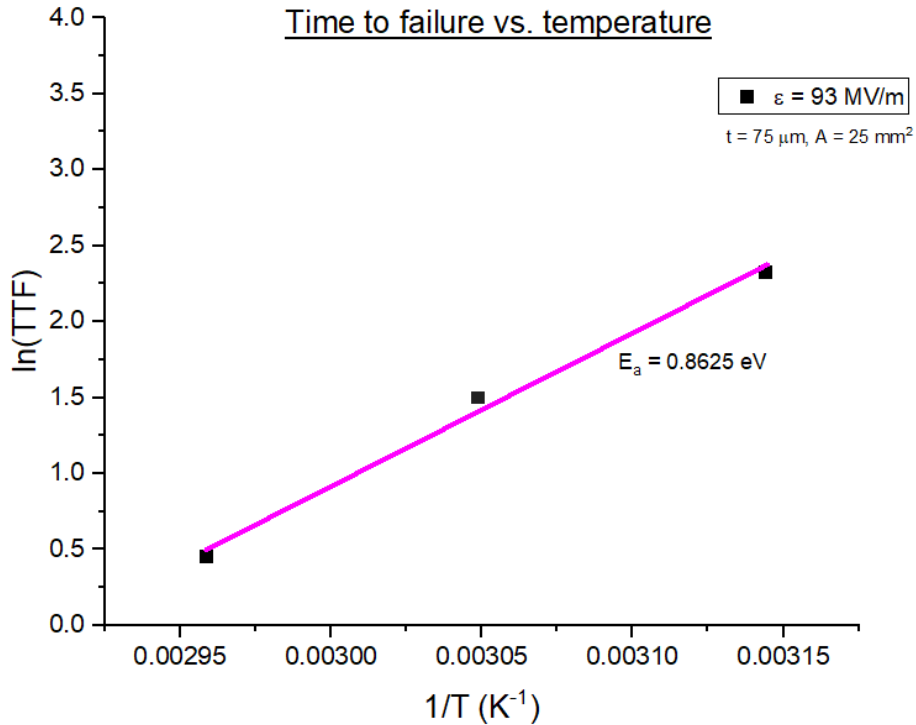


Figure 3-6 Time-to-failure vs. $1/T$ at $T = 318$ K, 328 K and 338 K

3.3.2.3. Lifetime prediction of capacitors using PVDF as a dielectric

To extrapolate the lifetime of capacitors with PVDF as a dielectric layer, the log time to failure vs. electric field applied is plotted and shown in Figure 3-7 for trial# 1-5, all at room temperature. The extrapolation is done based on the E-model as it provides the shortest time-to-failure out of the E, 1/E, and \sqrt{E} models and is assumed to be the most conservative. Two linear fits have been extrapolated. The first linear fit (a) includes all five data points and predicts a lifetime of 100,000 hours (~10 years) for an applied electric field of 40 MV/m. This equates to a capacitor voltage of 4000 V for a 100 μm thick dielectric layer. Linear fit (b) is extrapolated assuming trial #5 to be an outlier and indicates that the capacitor can be used for up to 100,000 hours (~ 10 years) under an electric field application of 92 MV/m. For a 100 μm thick dielectric layer, this equates to a capacitor voltage of 9200 V. Therefore, 4000 V – 9200 V can be considered as an operational range of capacitor voltage for the desired application.

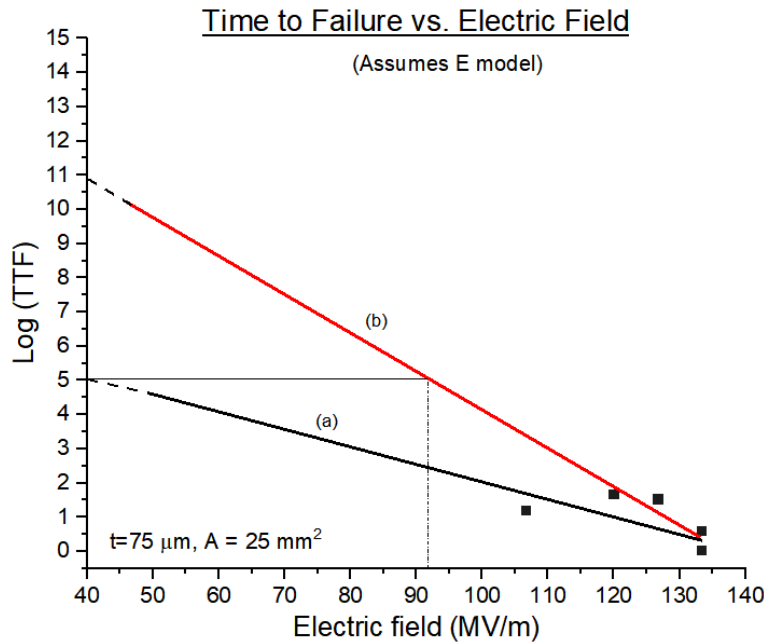


Figure 3-7 Plot of $\log(\text{time to failure})$ vs. electric field and extrapolation of lifetime assuming the 'E model' (a) Including all trials (#1-5) (b) excluding trial #5

CHAPTER 4: CONCLUSION AND FUTURE WORK

In this thesis, the DC dielectric breakdown strength of PVDF has been studied to understand its application as a potential dielectric material for roll-to-roll high energy density flexible capacitors. Stepped voltage ramp dielectric breakdown testing and time-dependent dielectric breakdown testing was performed to understand the withstanding capabilities and time-to-failure of PVDF by varying two main stress factors: voltage and temperature, while keeping the thickness and electrode area constant. From the results obtained in section 3.3, it can be concluded that PVDF does not breakdown under short time stepped voltage ramp tests up to 10 KV. From the time dependent dielectric breakdown tests, it is shown that the time-to-failure decreases with an increase in temperature as it leads to more heating and the defect generation process is quicker. The acceleration parameters were calculated at two different temperatures which are 0.04 and 0.08 $(\text{MV/m})^{-1}$ for temperatures corresponding to 318 K and 298 K respectively. The activation energy for the PVDF films was also calculated, which turns out to be 0.8625 eV. The lifetime prediction for the capacitors using PVDF as a dielectric material was done assuming the E model. The E model was chosen because it predicts the worst case and shortest time-to-failure and it follows an exponential dependence on the field and Arrhenius relationship with the temperature, where breakdown occurs due to bond ionization. The electric field proposed for a lifetime of 100,000 hours (10 years) was derived to be in the range of 40 - 92 MV/m which is equivalent to a capacitor voltage range of 4000 - 9200 V for a 100 μm dielectric film. Although the PVDF dielectric films can withstand up to 10 kV under short-time breakdown tests, they seem to be a promising candidate as a dielectric for energy storage applications at \sim 4 kV - 9 kV for a period of 10 years.

In addition, TDDB is a stochastic process and defect generation is random. To understand the long-term breakdown mechanism of PVDF films further, the effect of electrode size, shape and thickness of dielectric and metallization can be studied. It would be worthwhile to explore other polymer dielectrics such as polyethylene (PE) or polyethylene terephthalate (PET) as they also have been theoretically proposed to have high flexibility and dielectric breakdown strength. Moreover, PVDF has a limitation as it is not cost effective and the reduction of material cost for our application can also be investigated.

REFERENCES

- [1] “Lithium-ion Battery Pack Prices Rise for First Time to an Average of \$151/kWh.”
<https://about.bnef.com/blog/lithium-ion-battery-pack-prices-rise-for-first-time-to-an-average-of-151-kwh/> (accessed May 09, 2023).
- [2] R. Hafezi and M. Alipour, “Renewable Energy Sources: Traditional and Modern Age Technologies,” 2020, pp. 1–15. doi: 10.1007/978-3-319-71057-0_18-1.
- [3] L. Zhao and C. L. Liu, “Review and mechanism of the thickness effect of solid dielectrics,” *Nanomaterials*, vol. 10, no. 12. MDPI AG, pp. 1–24, Dec. 01, 2020. doi: 10.3390/nano10122473.
- [4] A. Von Rippel, “Electric Breakdown of~ Solid and Liquid Insulators.” [Online]. Available: http://pubs.aip.org/aip/jap/article-pdf/8/12/815/8050957/815_1_online.pdf
- [5] J. J. O’Dwyer, “Dielectric breakdown in solids,” *Adv Phys*, vol. 7, no. 27, pp. 349–394, 1958, doi: 10.1080/00018735800101297.
- [6] D. H. Frohlich, “THEORY OF DIELECTRIC BREAKDOWN*.”
- [7] S. Lombardo, J. H. Stathis, B. P. Linder, K. L. Pey, F. Palumbo, and C. H. Tung, “Dielectric breakdown mechanisms in gate oxides,” *Journal of Applied Physics*, vol. 98, no. 12. 2005. doi: 10.1063/1.2147714.
- [8] T. K. S. Wong, “Time dependent dielectric breakdown in copper low-k interconnects: Mechanisms and reliability models,” *Materials*, vol. 5, no. 9. pp. 1602–1625, 2012. doi: 10.3390/ma5091602.

- [9] J. R. Lloyd, E. Liniger, and T. M. Shaw, "Simple model for time-dependent dielectric breakdown in inter- and intralevel low- k dielectrics," *J Appl Phys*, vol. 98, no. 8, Oct. 2005, doi: 10.1063/1.2112171.
- [10] J. R. Lloyd, E. Liniger, and T. M. Shaw, "Simple model for time-dependent dielectric breakdown in inter- and intralevel low- k dielectrics," *J Appl Phys*, vol. 98, no. 8, Oct. 2005, doi: 10.1063/1.2112171.
- [11] J. W. Mcpherson and R. B. Khamankar, "Molecular model for intrinsic time-dependent dielectric breakdown in SiO₂ dielectrics and the reliability implications for hyper-thin gate oxide," 2000. [Online]. Available: <http://iopscience.iop.org/0268-1242/15/5/305>
- [12] J. W. Mcpherson and H. C. Mogul, "Underlying physics of the thermochemical E model in describing low-field time-dependent dielectric breakdown in SiO₂ thin films," 1998. [Online]. Available: http://pubs.aip.org/aip/jap/article-pdf/84/3/1513/6751716/1513_1_online.pdf
- [13] I. C. Chen, S. Holiand, and C. Hut, "A quantitative physical model for time-dependent breakdown in SiO₂."
- [14] C. H. Tung *et al.*, "Percolation path and dielectric-breakdown-induced-epitaxy evolution during ultrathin gate dielectric breakdown transient," *Appl Phys Lett*, vol. 83, no. 11, pp. 2223–2225, Sep. 2003, doi: 10.1063/1.1611649.
- [15] M. Leda, M. Nagao, and M. Hikita, "High-field Conduction and Breakdown in Insulating Polymers Present Situation and Future Prospects," 1004.

- [16] S. Li *et al.*, “Short-term Breakdown and Long-term Failure in Nanodielectrics: A Review,” 2010.
- [17] J. C. Fothergill, “Ageing, Space Charge and Nanodielectrics: Ten Things We Don’t Know About Dielectrics.” [Online]. Available: <http://openaccess.city.ac.uk/>
- [18] L. A. (Len A.) Dissado and J. C. (John C.) Fothergill, *Electrical degradation and breakdown in polymers*. P. Peregrinus, 1992.
- [19] R. Higgins and J. McPherson, “TDDDB evaluations and modeling of very high-voltage (10KV) capacitors,” in *IEEE International Reliability Physics Symposium Proceedings*, 2009, pp. 432–436. doi: 10.1109/IRPS.2009.5173292.
- [20] E. T. Ogawa, J. Kim, G. S. Haase, H. C. Mogul, and J. W. McPherson, “Leakage, breakdown, and TDDDB characteristics of porous low-k silica-based interconnect dielectrics,” in *IEEE International Reliability Physics Symposium Proceedings*, Institute of Electrical and Electronics Engineers Inc., 2003, pp. 166–172. doi: 10.1109/RELPHY.2003.1197739.
- [21] M. Hikita, M. Nagao, G. Sawat, and M. Ieda, “Dielectric breakdown and electrical conduction of poly(vinylidene-fluoride) in high temperature region,” 1980. [Online]. Available: <http://iopscience.iop.org/0022-3727/13/4/019>
- [22] L. Dou, Y. H. Lin, and C. W. Nan, “An overview of linear dielectric polymers and their nanocomposites for energy storage,” *Molecules*, vol. 26, no. 20. MDPI, Oct. 01, 2021. doi: 10.3390/molecules26206148.

- [23] S. Chisca, I. Sava, V. E. Musteata, and M. Bruma, “Dielectric and conduction properties of polyimide films,” in *Proceedings of the International Semiconductor Conference, CAS*, 2011, pp. 253–256. doi: 10.1109/SMICND.2011.6095784.
- [24] Q. G. Chi *et al.*, “Effects of magnetic field treatment on dielectric properties of CCTO@Ni/PVDF composite with low concentration of ceramic fillers,” *AIP Adv*, vol. 5, no. 11, Nov. 2015, doi: 10.1063/1.4935270.
- [25] D. Q. Tan, “Differentiation of roughness and surface defect impact on dielectric strength of polymeric thin films,” *IET Nanodielectrics*, vol. 3, no. 1, pp. 28–31, Mar. 2020, doi: 10.1049/iet-nde.2019.0031.
- [26] T. R. Jow and P. J. Cygan, “Dielectric breakdown of polyvinylidene fluoride and its comparisons with other polymers,” *Journal of Applied Physics*, vol. 73, no. 10, pp. 5147–5151, 1993. doi: 10.1063/1.353789.
- [27] M. Ieda, “DIELECTRIC BREAKDOWN PROCESS OF POLYMERS,” 1980.
- [28] G. Shimoga and S. Y. Kim, “High-k polymer nanocomposite materials for technological applications,” *Applied Sciences (Switzerland)*, vol. 10, no. 12, Jun. 2020, doi: 10.3390/app10124249.
- [29] “PVDF polyvinylidene fluoride resin (physical properties table 1) | KDA’s plastic processing technology.” https://www.kda1969.com/materials/pla_mate_pvdf2.htm (accessed Apr. 27, 2023).
- [30] “Plastic Rigidity & Material Stiffness.” <https://omnexus.specialchem.com/polymer-properties/properties/stiffness> (accessed Apr. 27, 2023).

- [31] M. M. Ueki and M. Zanin, "Influence of Additives on the Dielectric Strength of High-density Polyethylene," 1999.
- [32] D. E. Gray and B. H. Billings, *Properties of dielectrics*, 3rd ed. New York: McGraw-Hill, 1972.
- [33] "Overview of materials for Low Density Polyethylene (LDPE)."
https://www.matweb.com/search/datasheet_print.aspx?matguid=b34a78d271064c4f85f28a9ffaf94045 (accessed Apr. 27, 2023).
- [34] "Dielectric Constant of Selected Polymers."
https://hbcpc.chemnetbase.com/faces/documents/13_04/13_04_0001.xhtm (accessed Sep. 09, 2022).
- [35] S. J. Laihonen', "Influence of electrode area on dielectric breakdown strength of thin poly(ethylene terephthalate) films," 2004.
- [36] "Overview of materials for Polyimide."
<https://www.matweb.com/search/DataSheet.aspx?MatGUID=ab35b368ab9c40848f545c35bdf1a672&ckck=1> (accessed Apr. 27, 2023).
- [37] P. Saxena and P. Shukla, "A comprehensive review on fundamental properties and applications of poly(vinylidene fluoride) (PVDF)," *Advanced Composites and Hybrid Materials*, vol. 4, no. 1. Springer Science and Business Media B.V., pp. 8–26, Mar. 01, 2021. doi: 10.1007/s42114-021-00217-0.
- [38] W. Eisenmenger, H. Schmidt, and B. Dehlen, "Space Charge and Dipoles in Polyvinylidene fluoride," 1999.

- [39] W. Xia and Z. Zhang, "PVDF-based dielectric polymers and their applications in electronic materials," *IET Nanodielectrics*, vol. 1, no. 1. Institution of Engineering and Technology, pp. 17–31, 2018. doi: 10.1049/iet-nde.2018.0001.
- [40] S. Rajeevan, S. John, and S. C. George, "Polyvinylidene fluoride: A multifunctional polymer in supercapacitor applications," *Journal of Power Sources*, vol. 504. Elsevier B.V., Aug. 31, 2021. doi: 10.1016/j.jpowsour.2021.230037.
- [41] T. Wu *et al.*, "A flexible film bulk acoustic resonator based on β -phase polyvinylidene fluoride polymer," *Sensors (Switzerland)*, vol. 20, no. 5, Mar. 2020, doi: 10.3390/s20051346.
- [42] S. Rajeevan, S. John, and S. C. George, "Polyvinylidene fluoride: A multifunctional polymer in supercapacitor applications," *Journal of Power Sources*, vol. 504. Elsevier B.V., Aug. 31, 2021. doi: 10.1016/j.jpowsour.2021.230037.
- [43] "PVDF Film." <https://catalog.cshyde.com/viewitems/films/pvdf-kynar-film-polyvinylidene-fluoride> (accessed Sep. 19, 2022).
- [44] B. Mieller, "Influence of test procedure on dielectric breakdown strength of alumina," *Journal of Advanced Ceramics*, vol. 8, no. 2, pp. 247–255, Jun. 2019, doi: 10.1007/s40145-018-0310-4.
- [45] X. Wang, Z. D. Wang, C. Perrier, and S. Northcote, "ELECTRODE AREA EFFECT ON DIELECTRIC BREAKDOWN STRENGTHS OF MINERAL OIL AND ESTERS."

- [46] G. S. Haase, E. T. Ogawa, and J. W. McPherson, "Reliability analysis method for low- κ interconnect dielectrics breakdown in integrated circuits," *J Appl Phys*, vol. 98, no. 3, Aug. 2005, doi: 10.1063/1.1999028.
- [47] J. W. McPherson, "Time dependent dielectric breakdown physics - Models revisited," *Microelectronics Reliability*, vol. 52, no. 9–10, pp. 1753–1760, Sep. 2012, doi: 10.1016/j.microrel.2012.06.007.
- [48] M. Lin and K. C. Su, "Correlation between TDDB and VRDB for low- κ dielectrics with square root e model," *IEEE Electron Device Letters*, vol. 31, no. 5, pp. 494–496, May 2010, doi: 10.1109/LED.2010.2044554.
- [49] J. Mcpherson, V. Reddy, K. Banerjee, and H. Le, "Comparison of E and 1/E TDDB Models for SiO₂ under long-term high-field test conditions."
- [50] R. Higgins and J. McPherson, "TDDB evaluations and modeling of very high-voltage (10KV) capacitors," in *IEEE International Reliability Physics Symposium Proceedings*, 2009, pp. 432–436. doi: 10.1109/IRPS.2009.5173292.